

Atomic-Oxygen Durability of a Silicone Paint: Comparison Between Two Simulation Methods

I. Gouzman,^{*} E. Grossman,[†] G. Lempert,^{*} and Y. Noter[‡]

Soreq NRC, 81800 Yavne, Israel

Y. Lifshitz[§]

City University of Hong Kong, Hong Kong, People's Republic of China

and

V. Viel-Inguibert[¶] and M. Dinguirard^{**}

ONERA, F-31055 Toulouse, France

The present work summarizes durability tests of white antistatic silicone paint, SCK5, in a simulated low-Earth-orbit atomic-oxygen environment. Two types of the simulation systems were used: a plasma asher and a laser-detonation source producing a 5-eV atomic-oxygen beam. The SCK5-coated samples were also exposed to argon plasma, in order to separate between chemical effects of atomic oxygen and physical effects introduced by the plasma. A comparative study of the erosion yield, the surface morphology, and the chemical composition resulting from exposure to similar equivalent atomic-oxygen fluences in both types of simulation systems was performed. The SCK5 exposed to oxygen plasma showed significant cracking, whereas similar exposures to the 5-eV atomic-oxygen beam exhibited no cracking. In both cases the exposed samples showed a decrease of the carbon atomic concentration and an increase of the oxygen concentration in the upper surface layer. It is concluded that the erosion of SCK5 by the oxygen plasma is considerably more severe than by the 5-eV atomic oxygen, at least for the specific case of a porous silicic material, tested in the present work. The observed results are most probably associated with the nature of the reactive species in the plasma asher, their omnidirectional flux, and the high porosity of SCK5 coating.

Introduction

THE SCK5 white antistatic silicone paint was developed by Centre National d'Etudes Spatiales (CNES) and is manufactured by MAP (France) as a thermal control coating for high-frequency circuit materials.¹ This material has a very short shelf life (24 h), implying that the application should be done at the paint manufacturing site. Technically this can be achieved either by painting the surfaces at the plant or by purchasing a ready-made SCK5 painted Kapton film and adhering it to the surface of interest in the customer's facility.

The present work describes the ground testing of atomic-oxygen (ATOX) durability of different SCK5 painted surfaces, including a Kapton film, Duroid 5880 [a glass/Teflon[®] polytetrafluoroethylene (PTFE) composite], and TMM3 (a ceramic thermoset polymer composite).

The effects of ATOX, the most prominent hazard for polymeric materials in low Earth orbit (LEO), have been widely investigated in recent years by in-flight experiments as well as by laboratory simulation techniques.^{2–7} The difficulty of the ground simulation experiments to forecast the long-term LEO durability of external spacecraft materials stems from basic differences between the actual environment and the simulated one. These include 1) differences in

energy distribution and directionality of reactive species, 2) low ATOX flux in space as compared to accelerated tests, 3) neutral ground state ATOX in space as compared to ionic and excited species in some of the experiments, and 4) synergistic effects of ATOX, UV, and ionizing radiation in space.

Two different types of ground simulation techniques were used for simulation of the ATOX LEO environment in the present work. The first type included two rf plasma facilities. The rf plasma asher is a widely accepted simulation facility for screening tests in many laboratories.^{2,3} Plasma contains a mixture of reactive species (excited, neutral, and ionized oxygen atoms and molecules) that impinge upon the exposed surface omnidirectionally, as well as vacuum-UV (VUV) radiation. The source is capable of simulating high LEO equivalent ATOX fluences within reasonable experimental times. The second system was a laser detonation source. This source generates a highly directional, pulsed 5-eV ATOX beam accompanied by high doses of VUV radiation. The instantaneous ATOX flux during the pulse is four orders of magnitude larger than in the LEO environment, but the average value is similar to the LEO ATOX flux ($\sim 1 \times 10^{15}$ atoms/cm²s) (Refs. 4 and 5). A significant discrepancy between the results of the rf plasma and the laser detonation systems was observed in the present work, initiating detailed studies and reevaluation of both techniques.

Experimental Details

The tested samples included 1) Kapton coated with SCK5, further referred to as Kapton/SCK5; 2) Kapton coated with SCK5 and bonded by a pressure-sensitive adhesive to a Duroid 5880 (a glass/Teflon PTFE composite manufactured by Rogers Corporation) substrate, further referred to as Duroid/Kapton/SCK5; 3) Duroid 5880 coated directly with SCK5, further referred to as Duroid/SCK5; and 4) TMM3 (a ceramic/thermoset polymer composite, Rogers Corporation) coated directly with SCK5, further referred to as TMM3/SCK5.

A conventional rf plasma asher system (15 W, 13.56 MHz), operating at 100 mtorr, was used for most of rf plasma tests. The LEO equivalent ATOX flux in the central part of the RF plasma reactor was

Received 9 August 2002; revision received 20 February 2003; accepted for publication 8 August 2003. Copyright © 2003 by the American Institute of Aeronautics and Astronautics, Inc. All rights reserved. Copies of this paper may be made for personal or internal use, on condition that the copier pay the \$10.00 per-copy fee to the Copyright Clearance Center, Inc., 222 Rosewood Drive, Danvers, MA 01923; include the code 0022-4650/04 \$10.00 in correspondence with the CCC.

^{*}Senior Researcher, Materials Group, Space Environment Section.

[†]Head, Materials Group, Space Environment Section.

[‡]Head, Project Section, Space Environment Section.

[§]Professor, Department of Physics and Materials Science; on leave from Soreq NRC, 81800 Yavne, Israel.

[¶]Senior Researcher, Département Environnement Spatial, Centre d'Etudes et de Recherches de Toulouse.

^{**}Head of Department, Département Environnement Spatial, Centre d'Etudes et de Recherches de Toulouse.

$\sim 5 \times 10^{15}$ atoms/cm²s. The SCK5 coated samples were exposed to different ATOX fluences in the range from 2×10^{19} atoms/cm² to 1.7×10^{21} atoms/cm². Argon plasma was used to distinguish between chemical effects of atomic oxygen and physical effects introduced by the rf plasma.

A high-power rf plasma reactor (Litmas) was used to evaluate the relative effects of different plasma components, such as in-glow (all plasma components) and afterglow exposure, 100 mm away from the reactor (reduced amount of excited species, an increased amount of neutral atomic oxygen). A specially designed target holder assembly was used to eliminate the direct VUV irradiation allowing all other afterglow plasma components to react with the sample. The system was operated at 300 and 1200 W rf power at an oxygen pressure of 120 mtorr. The VUV flux was assessed by a phototube sensor positioned at the location of the exposed sample. The measurements were performed using a 1% transmission filter, in order to reduce the intensity to the working range of the sensor. The VUV flux was 1.6×10^{16} photons/cm²s at 300 W, 100 mm away from the reactor.

At Centre d'Etudes et de Recherches de Toulouse (CERT), samples were tested using a laser-detonation source [Chambre Adaptée à l'Action de l'Oxygène Atomique Sur les Revêtements (CASOAR), manufactured by PSI]. Under the operational conditions used in the present study, a mean LEO equivalent ATOX flux of $\sim 1 \times 10^{15}$ atoms/cm²s was obtained. A VUV flux of 1.85×10^{16} photons/cm²s was measured by a phototube detector. Modification of the CASOAR system allowed the separation between ATOX, VUV, and ATOX/VUV synergistic effects.⁸ Because of limitations of the system, only relatively low LEO equivalent ATOX fluences, amounting to 4×10^{19} atoms/cm² for ATOX without VUV and 2×10^{20} atoms/cm² for ATOX/VUV, were achieved. The samples were also exposed to VUV alone at a fluence of 2×10^{21} photons/cm².

In all ATOX simulation experiments the LEO equivalent atomic-oxygen fluence was evaluated by measuring the mass loss of a Kapton HN polyimide reference sample. The erosion rate of Kapton was assumed to be equal to 3×10^{-24} cm³/atom and independent of the ATOX fluence.⁹

The effects of ATOX exposure were studied by several complementary techniques including scanning electron microscopy (SEM), energy dispersive X-ray spectroscopy (EDS), and X-ray photoelectron spectroscopy (XPS). SEM micrographs were obtained using a FEI Quanta 200 microscope operating in the low vacuum mode. Surface elemental composition was estimated by means of EDS using a primary electron energy of 25 keV. To minimize surface charging effects, all samples were coated with a thin (~ 25 -nm) gold layer. The elemental composition and chemical bonding states in the near-surface region were assessed by XPS measurements. The measurements were carried out using a VG system with Mg K α (1253.5 eV) 200-W x-ray source and a triple channeltron 150-mm hemispherical analyzer, CLAM2.

Mass-loss measurements were carried out for all of the samples exposed in the laser-detonation system and for some samples exposed in the rf plasma asher system. The results were expressed in terms of the erosion yields of the SCK5 samples.

Results

Morphological Changes and Erosion Yields

RF Plasma Simulation

All types of SCK5 coated samples were exposed in a low-power rf plasma asher to different LEO equivalent ATOX fluences, ranging from $\sim 2 \times 10^{19}$ to 1.7×10^{21} atoms/cm².

Duroid/Kapton/SCK5. Duroid 5880 substrates (3×5 cm) were prepared, onto which SCK5 coated Kapton was adhered by a pressure-sensitive adhesive layer. The SCK5 coated Kapton was applied on both sides of the substrate in order to prevent its direct exposure to rf oxygen plasma. It was found that rf oxygen plasma exposure to ATOX fluence of 2×10^{20} atoms/cm² and higher resulted in well-distinguished changes in surface morphology, detected by the naked eye. The changes included the formation of numerous cracks on the initially smooth paint surface, resembling cracks in dry earth (Fig. 1a). Cracks were observed also at lower fluences, but they were hardly detected by the unaided eye. An average crack width

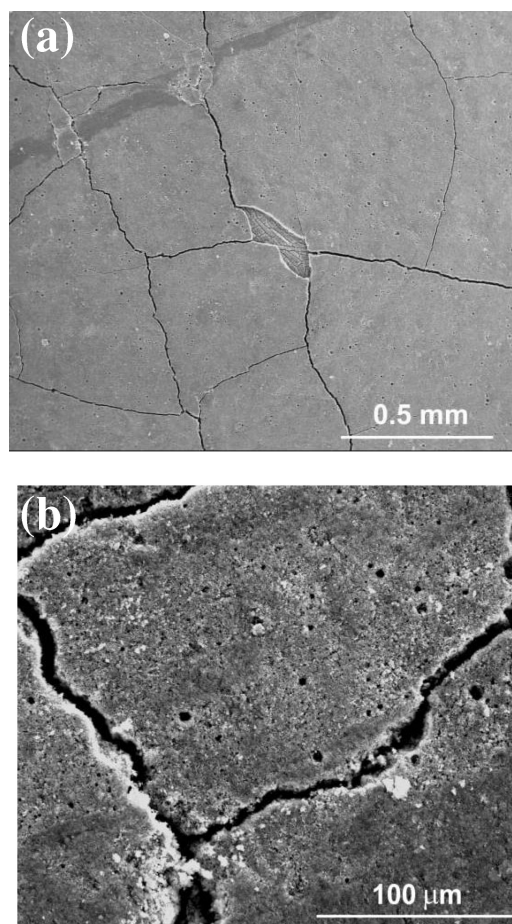


Fig. 1 SEM micrographs of Duroid/Kapton/SCK5 samples after exposure to rf oxygen plasma (1.0×10^{21} atoms/cm²): a) general view and b) magnified view of cracks.

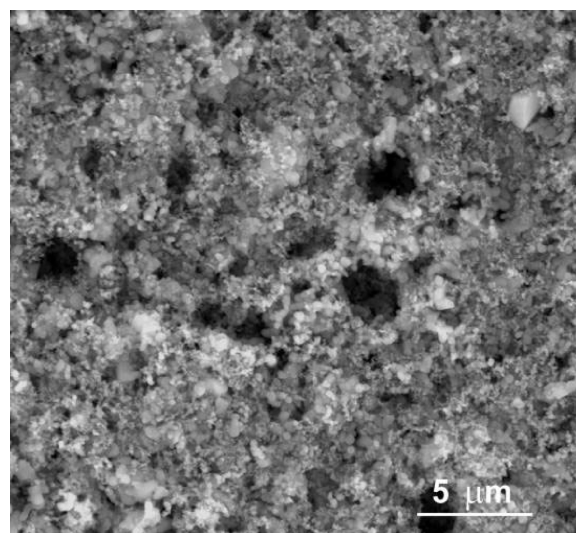


Fig. 2 SEM micrograph of an unexposed SCK5 coating.

of about $5 \mu\text{m}$ was estimated from SEM micrographs (Fig. 1b). The width, shape, and areal density of cracks did not change significantly with ATOX fluences above 2×10^{20} atoms/cm². The distance between cracks differed from about $100 \mu\text{m}$ to 1 mm. The morphology of the regions between the cracks was similar to that observed for unexposed samples (at the microscopic level used in this study). Note that the unexposed SCK5 coating was highly porous (Fig. 2). Pores with dimensions similar to the width of a crack were found

in the unexposed sample. The size and areal density of these pores did not change after ATOX exposure to different fluences.

Kapton/SCK5. A free-standing Kapton film ($\sim 40 \mu\text{m}$ thick, $1.5 \times 2.0 \text{ cm}$) painted with SCK5 was exposed in a low-power rf plasma asher to an ATOX fluence of about $\sim 5 \times 10^{19} \text{ atoms/cm}^2$. The sample was supported in a glass sample holder in order to reduce Kapton etching from the backside. After exposure, the sample was found to be strongly bent (upwardly concave). No cracks were found on the exposed surface by visual inspection. However, an attempt to flatten the bent film resulted in cracks. Because of the omnidirectional nature of the ATOX in the rf plasma system, it is difficult to expose only one side of the sample to ATOX and completely avoid the exposure of the backside. As Kapton itself undergoes erosion under ATOX exposure ($\sim 1.5 \mu\text{m}$ at $5 \times 10^{19} \text{ atoms/cm}^2$ of ATOX), the observed bending effect could be partially associated with a thinning of the peripheral part of the Kapton substrate, in addition to bending caused by ATOX-induced stresses in SCK5. To prevent Kapton erosion from the back side of the sample, additional experiment was performed in which Kapton/SCK5 sample was exposed in a special glass frame that maintained fixed position of the film. In this case well-defined cracks were observed on the SCK5 surface after ATOX exposure, similar to those shown in Fig. 1.

The erosion yield of the SCK5 was calculated using an ATOX fluence estimated from the mass loss of a Kapton witness sample exposed in the same experiment. The erosion yield was $\sim 5 \times 10^{-25} \text{ cm}^3/\text{atom}$ and $\sim 1 \times 10^{-24} \text{ cm}^3/\text{atom}$ after exposure to a LEO equivalent ATOX fluence of 3.6×10^{19} and $8 \times 10^{19} \text{ atoms/cm}^2$, respectively.

Duroid/SCK5. After exposure to the LEO equivalent ATOX fluence of about $2.5 \times 10^{19} \text{ atoms/cm}^2$, the initially smooth paint surface was cracked into well-distinguished domains. The size of an individual domain was approximately $1 \times 1 \text{ mm}$ (Fig. 3). The average width of the cracks was $5\text{--}7 \mu\text{m}$. However, because of the poor adhesion of the coating to the Teflon-based Duroid substrate many delaminated regions were observed, leading to the formation of the paint flakes. Note that the crack formation pattern is different for Duroid/Kapton/SCK5 and Duroid/SCK5 (see Figs. 1 and 3). It could be associated with the difference in surface structure and roughness of Kapton and Duroid substrates.

TMM3/SCK5. No cracks or other changes were observed by the naked eye after an ATOX exposure to a maximum fluence of $1.7 \times 10^{21} \text{ atoms/cm}^2$. However, SEM observations revealed cracks, similar to those shown in Fig. 1a. In this case neither delamination nor separation between substrate and coating were observed.

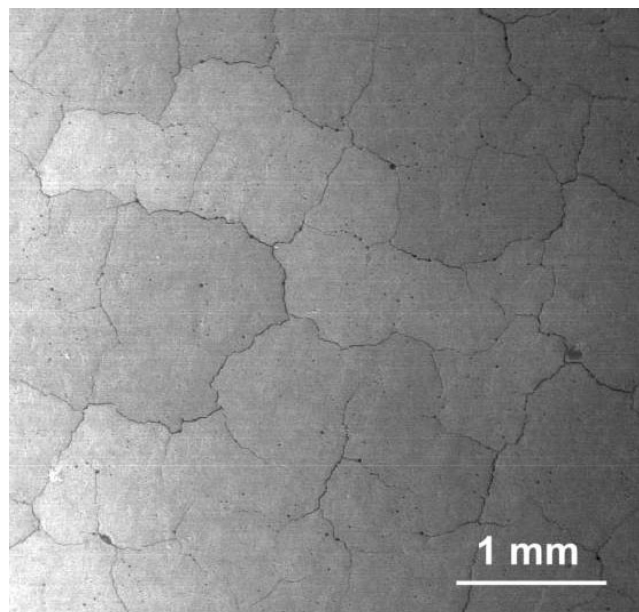


Fig. 3 SEM micrograph of the Duroid/SCK5 sample after exposure to $1.0 \times 10^{21} \text{ atoms/cm}^2$ of equivalent ATOX fluence (rf oxygen plasma simulation).

Argon rf plasma exposure. Three samples were subjected to argon rf plasma, including 1) a free-standing Kapton/SCK5 film, 2) a Kapton/SCK5 film in a glass frame, and 3) a Duroid/Kapton/SCK5. Cracks or bending of the Kapton/SCK5 film were not observed after Ar plasma exposure of all samples for 34 h, and the only effect was a very light coloration of the samples. (A 34-h exposure of rf oxygen plasma is equivalent to ATOX fluence of $6 \times 10^{20} \text{ atoms/cm}^2$.)

High-power rf plasma reactor. Dedicated experiments were carried out to distinguish between VUV and ATOX effects. This was achieved by using a high-power rf plasma apparatus and a specially designed target holder assembly located in the afterglow region. Kapton/SCK5 samples were exposed to 300 and 1200-W rf oxygen plasma afterglow flow including and excluding direct VUV radiation. In all cases similar cracking of the exposed area was observed after exposure to a LEO equivalent ATOX fluence of about $2 \times 10^{19} \text{ atoms/cm}^2$.

Laser-Detonation ATOX Source

Several samples of each type (Kapton/SCK5, Duroid/SCK5, TMM3/SCK5, and Duroid/Kapton/SCK5) were exposed simultaneously in the laser detonation 5-eV ATOX source (CASOAR). The samples were exposed to a LEO equivalent ATOX fluence of $4 \times 10^{19} \text{ atoms/cm}^2$, to synergistic ATOX/VUV fluences of $2 \times 10^{20} \text{ atoms/cm}^2$ and $2 \times 10^{21} \text{ photons/cm}^2$, respectively, and to a VUV fluence of $2 \times 10^{21} \text{ photons/cm}^2$. Surface morphology of the exposed samples was studied by SEM (data not shown). No cracks were found after the ATOX, ATOX/VUV, or VUV exposures. The erosion yields for Kapton/SCK5 exposed to various environments are shown in Table 1. The erosion yield was calculated using the LEO equivalent ATOX fluence obtained from the mass loss of Kapton witness samples exposed at the same time. The erosion yield of samples exposed to VUV was calculated using the VUV flux of $1.85 \times 10^{16} \text{ photons/cm}^2\text{s}$, as measured by a VUV detector.

Chemical Composition Changes

EDS Results

The elemental composition of SCK5 coated samples exposed in both simulation systems was determined by EDS, and the results are summarized in Table 2. The elemental composition of the reference sample (unexposed SCK5) was measured at several points to assess

Table 1 Erosion yields of Kapton/SCK5 samples exposed in the laser-detonation source

Environment	Fluence	Erosion yield
ATOX/VUV	$2 \times 10^{20} \text{ atoms/cm}^2$ and $2 \times 10^{21} \text{ photons/cm}^2$	$9.1 \times 10^{-26} \text{ cm}^3/\text{atom}$ (based on ATOX fluence)
VUV	$2 \times 10^{21} \text{ photons/cm}^2$	$1.3 \times 10^{-26} \text{ cm}^3/\text{photon}$
ATOX	$4 \times 10^{19} \text{ atoms/cm}^2$	$3.3 \times 10^{-25} \text{ cm}^3/\text{atom}$

Table 2 Elemental composition of SCK5 coated samples determined by EDS

Treatment	Element					
	C	O	Si	Ti	Zn	Sn
<i>Unexposed</i>						
Area I	21.3	46.1	6.5	9.8	7.1	9.2
Area II	19.6	48.1	6.7	9.7	6.9	9.0
<i>RF oxygen plasma</i>						
$2 \times 10^{19} \text{ atoms/cm}^2$	13.0	52.1	6.8	10.6	7.7	9.8
$9 \times 10^{19} \text{ atoms/cm}^2$	10.8	57.4	6.4	9.7	6.7	9.0
$1 \times 10^{21} \text{ atoms/cm}^2$	13.8	54.5	6.5	9.6	6.6	9.0
<i>Laser-detonation ATOX source</i>						
ATOX, $4 \times 10^{19} \text{ atoms/cm}^2$	15.0	50.7	7.4	10.3	7.0	9.6
ATOX/VUV, $2 \times 10^{20} \text{ atoms/cm}^2$ and $2 \times 10^{21} \text{ photons/cm}^2$	15.7	50.5	7.2	10.2	7.0	9.4

Table 3 Surface composition (at. %) determined from XPS data for Duroid/Kapton/SCK5 samples

Peak origin	Bonding state	Unexposed	CASOAR, ATOX, 4×10^{19} atoms/cm ²	CASOAR, ATOX/VUV, 2×10^{20} atoms/cm ²	RF plasma, 2×10^{19} atoms/cm ²	RF plasma, 1×10^{20} atoms/cm ²
Silicone matrix and contamination	C 1s	36.2	10.2	9.8	4.3	2.2
Silicone matrix, silicon oxide	Si 2p	24.1	30.5	30.4	23.7	23.9
Si-O-Si, metal oxides, SiO _x , adsorbed O, H ₂ O	O 1s	37.0	58.8	59.1	67.3	69.2
Metal oxides	Sn 3d, Zn 2p, Ti 2p	2.7	0.7	0.7	4.7	4.7

the uniformity of the coating. For all samples the most prominent effect was a decrease of carbon atomic concentration from about 20 at.% for the pristine coating to about 11–15 at.% after exposure to different fluences of ATOX. This was accompanied by an increase in oxygen atomic concentration in the analyzed layer. The modification of elemental composition in the analyzed region did not show a fluence dependence. No changes in Si, Ti, Zn, and Sn atomic concentrations were observed.

XPS Results

Chemical changes in the irradiated surface layer were detected by XPS. The following Duroid/Kapton/SCK5 samples were analyzed: an unexposed SCK5 coating, two samples exposed using the CASOAR system to ATOX/VUV and ATOX alone, respectively, as well as two samples exposed in a low power rf plasma asher to the LEO equivalent ATOX fluence of 2×10^{19} and 1×10^{20} O atoms/cm².

A typical XPS survey spectrum obtained from SCK5 surface included the Si 2p, C 1s, O 1s, Zn 2p, Sn 3d, and Ti 2p core level lines. High-resolution XPS spectra (not shown) obtained from the surfaces before and after exposure to various environments were used for chemical composition analysis. The near surface composition analysis was done by assuming that this region is homogeneous and using published atomic sensitivity factors.¹⁰ The results are presented in Table 3.

Discussion

The white paint SCK5 is a thermal control coating, applied on external satellite surfaces that can suffer from electrostatic discharge problems. The paint is composed of a purified silicone binder, “doped” metallic oxides that are responsible for its antistatic properties and white color appearance, aromatic solvents, and probably some other additives. One issue of primary importance for this coating is its atomic-oxygen durability. The SCK5 coatings (applied on Kapton, Duroid 5880, and TMM3) were tested using two types of ATOX simulation systems, an rf plasma asher, and a laser-detonation source.

RF oxygen plasma sources are commonly used for material screening with respect to ATOX degradation in LEO. The advantage of such a facility is its relatively low cost and simplicity. The source generates omnidirectional flux of oxygen atoms at thermal energies (~ 0.04 eV).³ However, other species are also present in the rf plasma environment, including molecular oxygen, atomic and molecular oxygen ions and electrons at energies of tens of eV, excited neutral and ionic species, as well as ~ 130 -nm VUV radiation with an approximate flux of 10^{13} – 10^{16} photons/cm²s (Refs. 11 and 12). The absolute and relative concentrations of these species depend crucially on the plasma operating conditions, such as plasma power, gas flow, pressure, chamber geometry, and the sample’s position inside the reactor. Therefore the plasma-surface interactions are extremely complex and might introduce various artifacts as compared to the real ATOX environment in LEO.

The laser-detonation atomic-oxygen source provides a highly directional beam of approximately 5-eV oxygen atoms. The mean flux provided by this source is about 1×10^{15} atoms/cm²s. However, the

atomic oxygen is generated in a pulsed mode, and the fluence in a single pulse can be as high as 1×10^{14} atoms/cm² in a period of time of about 100 μ s, which is equivalent to a flux of 1×10^{19} atoms/cm²s. This flux, higher by four orders of magnitude than in the LEO environment, might react differently with various materials, although as yet this is not supported by experimental evidence. The formation of atomic oxygen in a laser-detonation source is also accompanied by a high flux of VUV (1.85×10^{16} photons/cm²s). Therefore this source can provide a strong synergistic effect between ATOX and VUV. In the present study, a modification of the sample holder enabled separation of the ATOX beam from the VUV radiation. However, because of technical limitations the maximum ATOX fluence that could be simulated in this system within reasonable exposure time was far below the expected values in LEO applications.

The interactions of the isotropic, omnidirectional flux of thermal rf oxygen plasma vs the highly directional ATOX beam in LEO with uncoated and coated polymer surfaces were discussed by Banks et al.³ It was demonstrated that atomic-oxygen undercutting at defect sites (e.g., cracks) progresses much more rapidly in thermal energy plasma systems because of its omnidirectional impingement as compared to this effect in space. From this point of view, the ATOX interaction in the CASOAR simulation system resembles much more closely the LEO ram direction interaction. However, as was already noted, the very high instantaneous acceleration factor can introduce artifacts in the mechanism of chemical reaction and relaxation processes in ATOX-surface interactions.

The main visual effect of SCK5 exposure in the rf plasma simulation systems was its cracking. The cracking was observed after low equivalent ATOX fluence of about 2×10^{19} atoms/cm². Increasing the ATOX fluence beyond this value up to a maximum ATOX fluence of about 1.7×10^{21} atoms/cm² did not affect significantly the surface morphology. However, at some regions and for some materials delaminations of SCK5 were observed in the vicinity of the cracks at high ATOX fluences. This was most prominent for SCK5 coated Duroid substrates and Duroid/Kapton/SCK5 samples, where after exposure to rf oxygen plasma the SCK5 coating became brittle and was affected by vibrations and handling, causing formation of flakes. Such separated/delaminated fragments and flakes can act as a potential source of particulate contamination in space, which should be avoided. Microcracks in SCK5 could allow the penetration of ATOX and erosion of the underlying substrate by undercutting. It is noted that the cracks on the Kapton/SCK5, Duroid/SCK5, and Duroid/Kapton/SCK5 samples were readily observable by the naked eye, although their average width was only 5–7 μ m. Such narrow cracks are visible only in the case of a significant undercutting of the underlying substrate. In the case of TMM3 substrates coated with SCK5 and exposed to a maximum equivalent ATOX fluence of 1.7×10^{21} atoms/cm², no cracks were detected by the unaided eye. This can be explained by the better adhesion of SCK5 to TMM3, reducing SCK5 undercutting.

The observed results indicate a strong surface contraction of the SCK5 during interaction with rf oxygen plasma. Surface contraction leads to an increase of compressive stresses that finally result in fracture of the coating. In the case of a free-standing Kapton/SCK5 film, surface contraction caused the bending (concave upward) of the

flexible film and its cracking while attempting to flatten it, whereas fixed position of the film resulted in a stress relaxation via cracking during the ATOX exposure.

To separate between the chemical effects of atomic oxygen and possible artifacts of rf plasma caused by the electromagnetic field, UV radiation, electrons, and energetic ions, the SCK5 coated samples were exposed to a rf argon plasma. No cracks or other changes in surface morphology were found. Only some coloration was observed, probably associated with VUV exposure characteristic of rf plasma systems. Thus, the fracture and cracking of the SCK5 coating are clearly associated with oxygen reactivity.

The exposure of the various samples in the CASOAR system demonstrated milder changes, as compared to rf plasma systems. The only detected morphological effect was some slight bending of Kapton/SCK5 film. The same trend, namely, a milder deterioration of the SCK5 coating in the CASOAR system, was also reflected in the erosion yield and chemical composition results.

The observed erosion yields for the same type of tested samples differed for the rf plasma and the laser detonation sources. The erosion yield measured after exposure to various environments in a laser detonation source (CASOAR) was found to be dependent on the irradiation type. It was maximal in the case of ATOX exposure alone, less in the case of synergistic ATOX/VUV exposure, and minimal during exposure to VUV irradiation alone. The inhibiting effect of VUV is clearly observed from these results. Based on our previous studies,¹³ it is suggested that VUV radiation induces cross-linking in the silicic matrix, reducing the erosion rate caused by ATOX impingement and leading to a negative synergistic effect. For Kapton/SCK5 samples, the erosion yield was measured both after rf plasma and after laser-detonation source (CASOAR) treatments. The erosion yield after the rf plasma exposure was higher ($\sim 5 \times 10^{-25}$ and $\sim 1 \times 10^{-24}$ cm³/atom after exposure to a LEO equivalent ATOX fluence of 3.6×10^{19} and 8×10^{19} atoms/cm², respectively), compared to an ATOX or an ATOX/VUV irradiation in the CASOAR system ($\sim 3.3 \times 10^{-25}$ and $\sim 9.1 \times 10^{-26}$ cm³/atom after exposure to 4×10^{19} ATOX and 2×10^{20} atoms/cm² ATOX/VUV, respectively). The precise mass measurements of the exposed Kapton/SCK5 were problematic because of the unstable weight of the sample, probably as a result of humidity absorption by the exposed surfaces and/or charging problems.

Chemical composition of the SCK5 coating after exposure to rf plasma and laser-detonation sources was studied by EDS and XPS. The sampling depths of EDS are matrix dependent and lie within the range of 0.1 μ m for light elements, to about 3–5 μ m for some metals.¹⁴ XPS is a surface sensitive technique and probes the material to a depth of about 5 nm (Ref. 15). In addition, the sensitivity and accuracy of XPS measurements are higher as compared to EDS. The EDS and XPS analyses detected the following elements: C, O, Si, Ti, Zn, and Sn. Comparison of the EDS and XPS results indicated that the main changes induced by ATOX are localized in a thin layer at the surface. Besides, it was found that this layer is composed predominantly of organic matrix. This is because XPS analysis showed only small amounts of metals on the surface ($\sim 2.5\%$), whereas EDS revealed about 25% of Ti, Zn, and Sn. EDS studies did not reveal any significant changes in the metals and silicon concentrations after exposure to both rf plasma system and laser-detonation source, indicating that only a thin near-surface region is involved in the ATOX-material interaction. Note that the difference in surface morphology between rf plasma and laser-detonation source treated samples cannot be responsible for the difference in surface composition observed by XPS because the sampling area of the XPS is large (about 5×5 mm) compared to the areal density and width of the cracks.

Accurate quantitative analysis of chemical composition using XPS was problematic because of possible surface contamination, as well as high roughness and porosity of the SCK5. Particularly, the concentration of small metal-oxide particles embedded in the organic matrix can be affected by the surface morphology. In spite of these limitations, significant differences in the concentrations of different components were observed after exposure to 5-eV ATOX and rf oxygen plasma. The increase of Si atomic concentration (from

~ 24 at.% for unexposed sample to 30 at.%) in CASOAR experiment, concurrently with the decrease of carbon atomic concentration (from 36 to 10 at.%) and increase of oxygen atomic concentration (from ~ 37 to ~ 59 at.%), is associated with erosion of organic component and oxidation of siloxane into silicon oxide. In accordance with this model, O/Si ratio increases from 1.5 for unexposed paint to ~ 2 for samples exposed in the CASOAR system. Exposure to the rf oxygen plasma environment caused a drastic decrease in carbon atomic concentration as a result of isotropic arrival of atomic oxygen (see Table 3), accompanied by exposure of the metal-oxide particles and increase of the oxygen content (O/Si ~ 2.8). This can be explained, at least partially, by the adsorption of water vapor and oxygen from air. The data clearly indicate the higher deterioration of the SCK5 surface under rf exposure, supporting the surface morphology and erosion yields evidence.

Based on the preceding observations, the following phenomenological model is suggested. Cracking of the silicone-based SCK5 coating as a result of rf oxygen plasma is attributed to compressive stresses generated in the exposed coating because of a very effective erosion of the organic component in the silicone binder and formation of a brittle silicon oxide layer and strong surface contraction. Because of the omnidirectional character of atomic-oxygen impingement and the high porosity of SCK5 coating, this erosion process includes inner defects and pores. Consequently, a fast degradation of the silicone matrix takes place, leading to the exposure of the metal-oxide particles to the rf plasma. This model cannot be applied to the laser-detonation source because the generated ATOX interacts in a highly directional manner, creating a surface layer of silicon oxide, which might be noncontinuous and/or thinner than the rf-plasma-generated oxide layer and consequently less brittle.

It can be speculated that the interaction of the SCK5 coating with the rf plasma environment can also be affected by 1) electromagnetic field interaction with exposed metal oxide particles, 2) accompanying VUV irradiation, 3) electrons, and 4) energetic ions. To gain a deeper insight into the rf plasma-surface interactions, an experimental study has been initiated at Soreq NRC in order to understand in more detail the contributions, both individually and synergistically, of the different rf plasma components. Techniques have been developed to separate the plasma components in the plasma afterglow, where the effect of rf electromagnetic field is eliminated. This, however, did not prevent cracking of the SCK5 coating. In addition, a specially designed target holder assembly enabled the sample to be irradiated in the rf plasma afterglow, with and without direct VUV irradiation. No visible effect of the direct VUV flux on the surface morphology was observed.

Conclusions

Atomic-oxygen durability of SCK5 white antistatic silicone paint was studied using two types of simulation systems: a conventional rf oxygen plasma system and a laser-detonation oxygen source. The effects of equivalent atomic-oxygen-(ATOX) exposure on the surface morphology and surface composition of SCK5 coating applied on different substrates were studied by several complementary techniques, including scanning electron microscopy, energy-dispersive spectroscopy, and x-ray photoelectron spectroscopy. The tested materials were exposed to different equivalent atomic-oxygen fluences, ranging from 2×10^{19} up to 1.7×10^{21} atoms/cm².

The SCK5 exposed to rf plasma showed significant cracking, partial delamination, and enhanced embrittlement at a relatively low ATOX exposure. Similar samples exposed to the laser detonation source (5-eV ATOX) exhibited no cracking. The rf plasma simulation demonstrated a more severe degradation of SCK5 paint, evidenced by the morphological changes, as well as by erosion yields and chemical composition changes as compared to the laser detonation system. These results are most probably associated with a combination of omnidirectional flux of reactive species and high porosity of SCK5 coating, which result in strong compressive stresses and consequently cracking of the brittle silicon-oxide layer. It is suggested that rf oxygen plasma overestimates the ATOX interactions in low Earth orbit, at least for the specific case of a porous coating of silicic material, tested in the present work.

References

- ¹Guérard, F., and Guillaumont, J. C., "Thermal Control Paints and Various Materials for Space Use," *Proceedings of the 7th International Symposium on Materials in a Space Environment*, ESA SP 399, Noordwijk, The Netherlands, 1997, pp. 457, 458.
- ²Golub, M. A., Wydeven, T., and Cormia, R. D., "ESCA Study of Kapton Exposed to Low Earth Orbit or Downstream from a Radio-Frequency Oxygen Plasma," *Polymer Communications*, Vol. 29, Oct. 1988, pp. 285–288.
- ³Banks, B. A., de Groh, K. K., Rutledge, S. K., and DiFilippo, F. J., "Prediction of In-Space Durability of Protected Polymers Based on Ground Laboratory Thermal Energy Atomic Oxygen," NASA 107209, April 1996.
- ⁴Caledonia, G. E., Krech, R. H., and Green, B. D., "A High Flux Source of Energetic Oxygen Atoms for Material Degradation Studies," *AIAA Journal*, Vol. 25, No. 1, 1987, pp. 59–63.
- ⁵Caledonia, G. E., Krech, R. H., Oakes, D. B., Lipson, S. J., and Blumberg, W. A. M., "Products of the Reaction of 8 km/s N(⁴S) and O₂," *Journal of Geophysical Research*, Vol. 105, No. A6, 2000, pp. 12,833–12,837.
- ⁶Minton, T. K., and Garton, D. J., "Dynamics of Atomic-Oxygen-Induced Polymer Degradation in Low Earth Orbit," *Chemical Dynamics in Extreme Environments: Advanced Series in Physical Chemistry*, edited by R. A. Dressler, 1st ed., World Scientific, Singapore, 2001, pp. 420–489.
- ⁷Koontz, S. L., Albyn, K., and Leger, L. J., "Atomic Oxygen Testing with Thermal Atom Systems: a Critical Evaluation," *Journal of Spacecraft and Rockets*, Vol. 28, No. 3, 1991, pp. 315–323.
- ⁸Grossman, E., Gouzman, I., Viel-Inguibert, V., and Dinguirard, M., "Modification of a 5-eV Atomic Oxygen Laser Detonation Source," *Journal of Spacecraft and Rockets*, Vol. 40, No. 1, 2003, pp. 110–113.
- ⁹Minton, T. K., "Protocol for Atomic Oxygen Testing of Materials in Ground Based Facilities," Ver. 2, Jet Propulsion Lab., Publication 95-17, Pasadena, CA, Sept. 1995.
- ¹⁰Moulder, J. F., Stickle, W. F., Sobol, P. E., and Bomben, K. D., *Handbook of X-Ray Photoelectron Spectroscopy*, edited by J. Chastain and R. C. King Jr., Physical Electronics, Inc., Eden Prairie, MN, 1995.
- ¹¹Townsend, J. A., "A Comparison of Atomic Oxygen Degradation in Low Earth Orbit and in a Plasma Etcher," *Proceedings of the 19th Space Simulation Conference*, NASA CP 3341, 1996, pp. 249–258.
- ¹²Kearns, D. M., Gillen, D. R., Voulot, D., McCullough, R. W., Thompson, W. R., Cosimini, G. J., Nelson, E., Chow, P. P., and Klaassen, J., "Study of the Emission Characteristics of RF Plasma Source of Atomic Oxygen: Measurements of Atom, Ion, and Electron Fluxes," *Journal of Vacuum Science and Technology A*, Vol. 19, No. 3, 2001, pp. 993–997.
- ¹³Grossman, E., Noter, Y., and Lifshitz, Y., "Oxygen and VUV Irradiation of Polymers: Atomic Force Microscopy (AFM) and Complementary Studies," *Proceedings of the 7th International Symposium on Materials in a Space Environment*, ESA SP-399, Noordwijk, The Netherlands, 1997, pp. 217–223.
- ¹⁴Goldstein, J. I., Newbury, D. E., Echlin, P., Joy, D. C., Roming, A. D., Jr., Lyman, C. E., Fiori, C., and Lifshin, E., *Scanning Electron Microscopy and X-Ray Microanalysis*, 2nd ed., Plenum, New York, 1992, Chap. 3.
- ¹⁵Walls, J. M., *Methods of Surface Analysis*, Cambridge Univ. Press, 1990, p. 94.

D. Edwards
Associate Editor

Economic Principles Applied to Space Industry Decisions

Joel S. Greenberg, Princeton Synergetics, Inc.



This is not an economics book. It is a book about the application of economic principles and concepts in decision making related to space activities. The book is primarily tutorial and elaborates upon concepts and methodology and their applications. Emphasis is placed upon applications with typical results of performed analyses presented to demonstrate concepts and methods.

The use of mathematical and simulation models serves as the underpinning for much of the presented materials. The specific models considered have been selected to demonstrate the role that a structured thought process can play in the decision process. Since most decisions relating to technology development, product design, capital expenditures, and investments involve uncertainty and risk, a number of the selected models, developed methodologies, and presented examples explicitly and quantitatively consider uncertainty and risk.

The objective of this book is to put economic analysis into perspective with respect to real-world decision making in the space industry. It will expand the perspective of the reader with respect to the type of tools and analyses that might be brought to bear on complex business and government problems.

Contents:

Introduction • Investment Decisions • RLV Economics • Space Operations • Licensing and Regulatory Issues • Beyond Space: Energy and Gaming • Appendix: Estimating the Likelihood of Investment

Progress in Astronautics and Aeronautics Series

2003, 480 pages, Hardback

ISBN: 1-56347-607-X

List Price: \$100.95

AIAA Member Price: \$69.95

Publications Customer Service, P.O. Box 960

Herndon, VA 20172-0960

Phone: 800/682-2422; 703/661-1595

Fax: 703/661-1501

E-mail: warehouse@aiaa.org • Web: www.aiaa.org



American Institute of
Aeronautics and Astronautics